Journal of Hazardous Materials 161 (2009) 1338–1346

Contents lists available at ScienceDirect

Journal of Hazardous Materials

journal homepage: www.elsevier.com/locate/jhazmat

The role of electronic properties to the mutagenic activity of 1,6- and 3,6-dinitrobenzo[*a*]pyrene isomers

Vito Librando*, Andrea Alparone

Research Centre for Analysis, Monitoring and Minimization Methods of Environmental Risk and Department of Chemistry, University of Catania, viale A. Doria 8, I-95125 Catania, Italy

ARTICLE INFO

Article history:
Received 6 March 2008
Received in revised form 22 April 2008
Accepted 23 April 2008
Available online 1 May 2008

Keywords:
Dinitrobenzo[*a*]pyrenes
Nitropolycyclic aromatic hydrocarbons
Mutagenicity
Dipole moment
Density Functional Theory

ABSTRACT

Equilibrium geometries, infrared spectra, vertical first ionization potential (IP), electronic affinity (EA), dipole moment (μ) and electronic dipole polarizability (α) of 1,6- and 3,6-dinitrobenzo[*a*]pyrene isomers (1,6-DNB*a*P and 3,6-DNB*a*P) were evaluated by means of Density Functional Theory (DFT) and recent semiempirical PM6 method. Structural, energetic and vibrational properties of DNB*a*P isomers are substantially similar to each other. Calculated IP, EA and α values of these isomers are practically identical, while μ of 3,6-DNB*a*P (8.2 D at DFT level) is predicted to be ca. 4 times the value of 1,6-DNB*a*P isomer (1.9 D at DFT level), owing to favorable mutual orientation of the individual nitro group vectors. Higher direct-mutagenic activities of 3,6-DNB*a*P with respect to 1,6-DNB*a*P isomer by 1–2 orders of magnitude might be determined by its peculiar electronic charge distribution, which through stronger electrostatic and inductive interactions, can promote much more effectively binding to active-site of enzymes involved in mutagenic pathways. On the other hand, orientation of the nitro substituents relatively to the plane of the aromatic moiety, molecular sizes, as well as nitroreduction and oxidation reactions seem not to have a key role in the determination of the different mutagenic behaviour of these isomers.

1. Introduction

It is well known that many nitropolycyclic aromatic hydrocarbons (NPAHs) are contaminants potentially hazardous for public health due to their persistency in the environment and high mutagenic and carcinogenic activities [1–3]. NPAHs are usually generated from nitration reactions during combustion processes and also from reactions in atmosphere between polycyclic aromatic hydrocarbons (PAHs) and nitrogen oxides, contributing to polar fractions of airborne matter [1–6]. It is recognized that NPAHs are chemically and biochemically very stable species [7]. Besides traditional methods for remediation from polluted sites, novel strategies for the treatment and biodegradation of these compounds make use of specific bacterial enzymes [7–9]. Proposed mutagenic mechanisms of NPAHs are rather complex and depend on the environmental conditions, involving diffusional pathways in the cellular systems, binding to active-site of enzymes, oxidation and/or reduction reactions or their combinations [2,3,10,11]. Additionally, other contributions such as hydrophobic character, metabolic activity, efficient intercalation into DNA and group orientation prior to binding may rule the capability of metabolites to bind covalently to DNA and consequently the mutagenic behaviour [12]. It is widely documented in the literature that mutagenic potency of NPAHs is dependent on the molecular structure [3,13], which may also affect other critical physicochemical properties involved in mutagenic pathways. Geometrical features, in particular the angle of the plane of the nitro substituent formed with the plane of the aromatic system influence significantly the biochemical activity [3,13]. There are many indications showing that, NPAH isomers with the nitro group perpendicular or nearly perpendicular to the plane of the aromatic moiety exhibit lower mutagenic activity than planar or nearly planar homologues, in many cases with differences of some orders of magnitude [3,13]. This fact has been explained on the basis of orientation of the nitro substituents, which is supposed to control the access and occupation of the active-site of the nitroreductase enzyme [12,14].

In the case of dinitrobenzo[*a*]pyrenes (DNB*a*P), direct-mutagenic activities of two isomers, 1,6-DNB*a*P and 3,6-DNB*a*P, obtained through *Salmonella typhymurium* strains TA98 and YG1024 in the absence of metabolic activation system (S9) were investigated [15–18]. The results of both the tests concordantly show that 3,6-DNB*a*P exhibits substantially higher mutagenic potencies than those for 1,6-DNB*a*P isomer. Specifically, mutagenic activities for 3,6-DNB*a*P isomer are predicted to be 137,000 and

* Corresponding author. Tel.: +39 95 7385201; fax: +39 95 580138.
E-mail address: vlibrando@unict.it (V. Librando).

0304-3894/$ – see front matter © 2008 Elsevier B.V. All rights reserved.
doi:10.1016/j.jhazmat.2008.04.095

1,640,000 revertants/nmol, by TA98 and YG1024 strains, respectively, while the corresponding figures for 1,6-DNB*a*P isomer are much more lower, being 1514 and 82,593 revertants/nmol, respectively [18]. These findings are also supported by the fact that in the case of 3,6-DNB*a*P isomer, reduction reactions yield a larger amount of nitroso- and amino-derivative products than 1,6-DNB*a*P isomer [18]. Additionally, according to tests on F344/DuCrj rats, 3,6-DNB*a*P is demonstrated to be more carcinogenic than 1,6-DNB*a*P isomer [19]. Due to the presence of two withdrawal nitro substituents, 3,6-DNB*a*P is predicted to be more mutagenic than nitrobenzo[*a*]pyrenes (NB*a*P) [15–18,20]. However, owing to their high sensitivity to UV radiations, detection in the environment of DNB*a*Ps is a hard task [21]. Hitherto, experimental and theoretical structural data of DNB*a*Ps are not available, while X-ray structure of 6-NB*a*P [22] and Density Functional Theory (DFT) [23] geometries of 1-, 3- and 6-NB*a*P isomers [24] have been recently obtained. It is well established that nearly planar 1-NB*a*P and 3-NB*a*P are more mutagenic than the quasi-orthogonal 6-NB*a*P isomer [15–18,20].

In this work we focused our attention on the structure, infrared spectra and some fundamental physicochemical properties such as ionization potential (IP), electron affinity (EA), dipole moment (μ) and electronic dipole polarizability (α) of 1,6-DNB*a*P and 3,6-DNB*a*P isomers, to investigate the effects of the position of the nitro groups on these properties. The main aim is to elucidate the role of the structural and electronic properties in determination of the different mutagenic behaviour of these isomers. To this purpose, we used DFT and semiempirical computational methods. Recently, DFT electronic polarizabilities have been employed with success in the prediction of biodegradation rates of a series of dimethylnaphthalene isomers [25].

2. Computational methods

All calculations were performed with MOPAC 2007 [26] and GAUSSIAN 03 [27] series of programs. Equilibrium geometries were fully optimized by recent semiempirical PM6 method [28] as well as DFT-B3LYP functional [29,30] with the polarized split-valence Pople's 6-31G* basis set [31]. Infrared spectra were calculated at the B3LYP/6-31G* level on the B3LYP/6-31G* geometry under the harmonic approximation. Vibrational analysis showed that all the structures are minima in the potential energy surface (no imaginary frequencies).

Vertical first IP and EA values were obtained at the B3LYP/6-31+G* level through a ΔSCF procedure:

$$\mathrm{IP} = E_{\mathrm{cation}} - E_{\mathrm{neutral}} \quad (1)$$

$$\mathrm{EA} = E_{\mathrm{neutral}} - E_{\mathrm{anion}} \quad (2)$$

where E_{cation}, E_{neutral} and E_{anion} is single point total energy of the cation, neutral and anion state, respectively, at the B3LYP/6-31G* optimized geometry of the neutral ground state. For the investigated DNB*a*P isomers, 6-31+G* basis set, which contains polarized *d* and diffuse *s* and *p* functions on carbon, nitrogen and oxygen atoms, which are necessary to properly describe the electronic structure of radical ionic states, consists of a total of 514 basis functions. For both open-shell cations and anions we adopted unrestricted functional (UB3LYP), while for the closed-shell neutral ground state the restricted method (RB3LYP) was employed. In the present case, UB3LYP scheme was able to remove a large percentage of the spin contamination from the pseudo wavefunction ($S^2 \sim 0.75$). Recently, Modelli et al. have employed UB3LYP/6-31+G* level of calculation to obtain the EA values for many PAHs [32] and isothiocyanates [33], reproducing satisfactorily experimental data.

Atomic charges were estimated through atomic polar tensor (APT) [34,35], Mulliken [31], Merz-Singh-Kollman electrostatic potential (ESP) [36] and natural bond order (NBO) [37] population analyses.

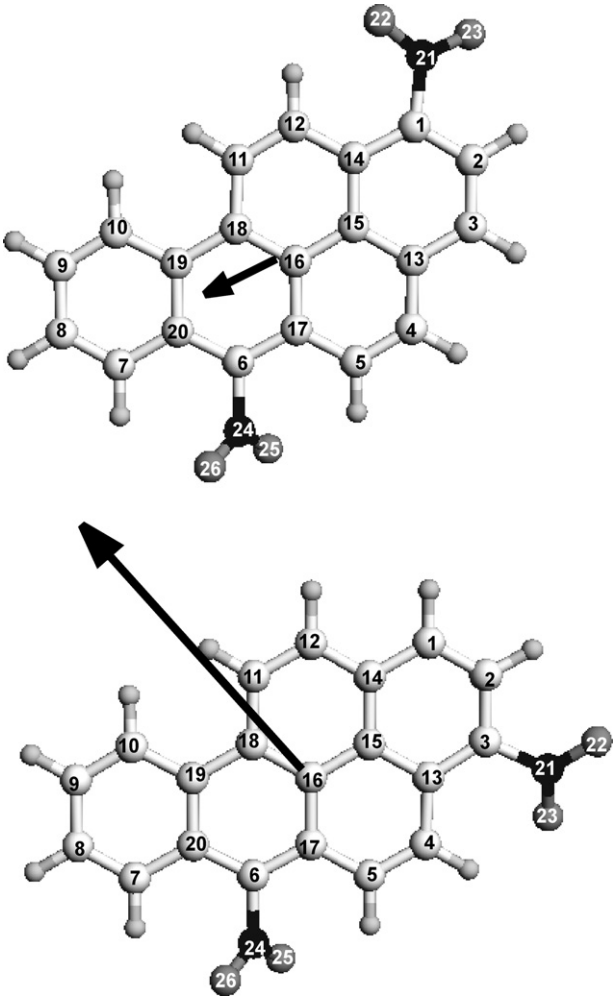

Fig. 1. Structure, atomic numbering and dipole moment vector of dinitrobenzo[*a*]pyrenes.

Dipole moment components (μ_i) of the neutral ground state were obtained at the PM6 and B3LYP/6-31+G* levels as first-order derivatives of the energy (E) with respect to the Cartesian coordinate components of the electric field (F_i), while static electronic polarizability tensor components (α_{ij}) were computed by the PM6 method as second-order derivative of E [38,39]. In experiments, polarizability is usually given as orientationally averaged value (<α>) [39].

Conversion factors to SI units are: energy (E), 1 Hartree = $4.3597482 \times 10^{-15}$ J; dipole moment (μ), 1 D = 3.33564×10^{-30} cm; dipole polarizability (α), 1 a.u. = 1.648778×10^{-41} C^2 m^2 J^{-1}.

3. Results and discussion

3.1. Geometries

Selected geometrical parameters of the nitro groups of the DNB*a*P isomers obtained at the B3LYP/6-31G* and PM6 levels are listed in Table 1 and the structures are displayed in Fig. 1. To our knowledge both experimental and theoretical data on the structure of DNB*a*Ps are lacking. Table 1 also reports the geometries of benzo[*a*]pyrene (B*a*P), for which observed data are available from X-ray measurements [40]. The results show that, despite the presence

Table 1
Selected geometrical parameters of dinitrobenzo[*a*]pyrene isomers and benzo[*a*]pyrene

Parameter[a]	1,6-DNB*a*P		3,6-DNB*a*P		B*a*P		
	B3LYP/6-31G*	PM6	B3LYP/6-31G*	PM6	B3LYP/6-31G*	PM6	Experimental[b]
C_1–C_2	1.391	1.399	1.378	1.379	1.388	1.386	1.383
C_2–C_3	1.388	1.396	1.401	1.416	1.399	1.407	1.399
C_3–C_{13}	1.399	1.397	1.411	1.403	1.399	1.393	1.395
C_{13}–C_{15}	1.429	1.428	1.436	1.434	1.431	1.430	1.443
C_{14}–C_{15}	1.434	1.424	1.427	1.419	1.426	1.418	1.421
C_1–C_{14}	1.422	1.420	1.409	1.415	1.410	1.415	1.408
C_4–C_{13}	1.436	1.456	1.440	1.457	1.442	1.459	1.441
C_4–C_5	1.355	1.349	1.357	1.348	1.357	1.350	1.345
C_5–C_{17}	1.442	1.461	1.439	1.459	1.442	1.460	1.451
C_{16}–C_{17}	1.444	1.444	1.441	1.444	1.442	1.445	1.445
C_{15}–C_{16}	1.435	1.448	1.435	1.447	1.430	1.443	1.443
C_{12}–C_{14}	1.429	1.444	1.425	1.444	1.428	1.444	1.444
C_{11}–C_{12}	1.365	1.357	1.364	1.353	1.366	1.360	1.354
C_{11}–C_{18}	1.427	1.445	1.430	1.446	1.432	1.445	1.436
C_{16}–C_{18}	1.417	1.405	1.420	1.406	1.419	1.405	1.420
C_6–C_{17}	1.391	1.389	1.391	1.388	1.384	1.377	1.376
C_6–C_{20}	1.422	1.437	1.421	1.436	1.414	1.429	1.421
C_{18}–C_{19}	1.442	1.439	1.443	1.440	1.443	1.442	1.456
C_{19}–C_{20}	1.434	1.421	1.434	1.420	1.435	1.419	1.419
C_7–C_8	1.374	1.372	1.374	1.372	1.375	1.372	1.377
C_8–C_9	1.412	1.423	1.412	1.423	1.414	1.424	1.423
C_9–C_{10}	1.376	1.372	1.376	1.372	1.378	1.373	1.379
C_{10}–C_{19}	1.420	1.431	1.421	1.431	1.421	1.430	1.428
C_7–C_{20}	1.424	1.432	1.424	1.432	1.423	1.431	1.429
N_{21}–C_1	1.471	1.482					
N_{21}–C_3			1.472	1.483			
N_{24}–C_6	1.475	1.486	1.475	1.487			
N_{21}–O_{22}	1.234	1.220	1.232	1.221			
N_{21}–O_{23}	1.232	1.221	1.233	1.220			
N_{24}–O_{25}	1.231	1.220	1.230	1.219			
N_{24}–O_{26}	1.230	1.218	1.231	1.218			
O_{22}–N_{21}–C_1–C_{14}	25.3	18.8					
O_{23}–N_{21}–C_1–C_2	24.0	17.9					
O_{22}–N_{21}–C_3–C_2			25.8	17.2			
O_{23}–N_{21}–C_3–C_{13}			27.6	18.1			
O_{25}–N_{24}–C_6–C_{17}	57.1	48.5	57.1	49.5			
O_{26}–N_{24}–C_6–C_{20}	56.9	48.8	56.9	49.7			

B3LYP/6-31G*and PM6 results.
[a] Bond lengths (Å), angles in degrees. See Fig. 1 for atomic numbering.
[b] X-ray diffraction C—C bond lengths taken from Ref. [40].

of solid-state effects, both the B3LYP/6-31G* and PM6 gas-phase geometries of B*a*P are in reasonable agreement with the experimental one, with a root-mean squared (rms) deviation for the C—C bond lengths of 0.009 and 0.008 Å, respectively. Introduction of nitro groups to the B*a*P moiety gives only a marginal alteration of the structure. Indeed, the aromatic rings remain substantially planar, the largest C—C—C—C dihedral angle being computed to be 3°. In addition, rms deviations of only 0.004–0.005 Å from the computed C—C bond lengths of B*a*P are found.

For 1,6-DNB*a*P isomer at the B3LYP/6-31G* level of calculation, the O—N—C—C dihedral angles for the nitro group in position 1 are computed to be 25° (O_{22}–N_{21}–C_1–C_{14}) and 24° (O_{23}–N_{21}–C_1–C_2), which are somewhat close to the values for the nitro group in position 3 for 3,6-DNB*a*P isomer, being 26° (O_{22}–N_{21}–C_3–C_2) and 28° (O_{23}–N_{21}–C_3–C_{13}). Note that, the corresponding O—N—C—C values for the nitro group in position 6 (O_{25}–N_{24}–C_6–C_{17} and O_{26}–N_{24}–C_6–C_{20}) are about doubled (57° for both isomers) in comparison to those in 1 and 3 positions, owing to the noticeable steric repulsion between the hydrogen atoms in peri position and vicinal oxygen atoms. Analogue results have been recently obtained on 1-, 2- and 9-nitroanthracene isomers [41] and 1-, 3- and 6-NB*a*P isomers [24] by using B3LYP computations. As can be seen in Table 1, for both DNB*a*P isomers, N_{24}–C_6 bond length is longer than N_{21}–C_1 and N_{21}–C_3 values by 0.003–0.004 Å, consistently with the O—N—C—C data. By contrast, N—O distances of nitro groups in 1 and 3 positions are slightly longer than those in position 6. Therefore, nitro group in position 6 exhibits a lower π-conjugation with the B*a*P moiety in comparison to that in 1 and 3 positions. As for O—N—C—C dihedral angles, N—O, N—C and C—C bond lengths for DNB*a*P isomers are rather similar to each other, suggesting that the investigated isomers exhibit a somewhat similar structure. It reflect on the relative stability, 3,6-DNB*a*P lying only 0.56 and 0.49 kcal/mol above 1,6-DNB*a*P isomer, respectively, at the B3LYP/6-31G* and PM6 levels. Note that, introduction of zero-point vibrational energy correction estimated at the B3LYP/6-31G* level under the harmonic approximation does not modify the relative stability. In addition we notice that, on passing from 1,6-DNB*a*P to 3,6-DNB*a*P isomer the molar volume determined by means of a Monte-Carlo procedure using a 0.001 e/bohr^3 density envelope decreases by only 4%. Our data indicate that, the geometrical features of the nitro groups of 1,6-DNB*a*P and 3,6-DNB*a*P isomers being somewhat similar are expected not to be decisive in determining their different mutagenic activity.

3.2. Infrared spectra

Infrared spectrum of DNB*a*P isomers was computed at the B3LYP/6-31G* level under the harmonic approximation. B3LYP functional have been previously employed with success in determination of vibrational spectra of nitroaromatic molecules [24,42,43].

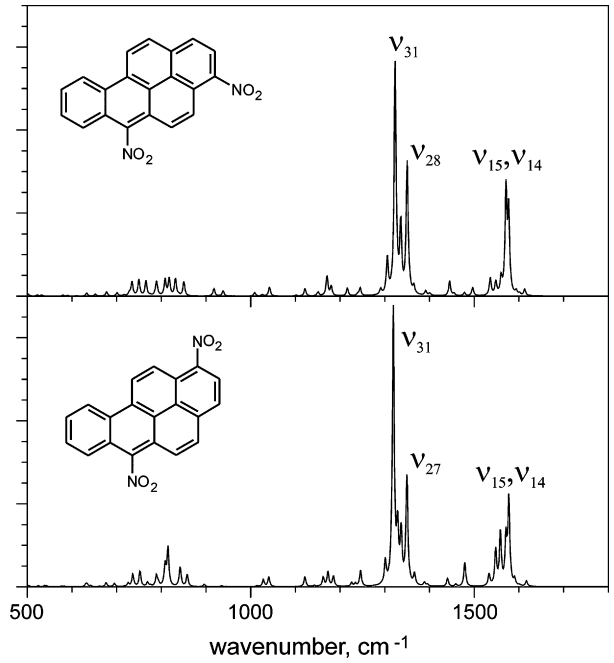

Fig. 2. B3LYP/6-31G* infrared spectrum in the 500–1800 cm^{-1} range of 1,6-dinitrobenzo[*a*]pyrene (bottom) and 3,6-dinitrobenzo[*a*]pyrene (top) isomers. Wavenumbers were corrected by 0.9594 scaling factor taken from Ref. [46]. Lorentz lineshapes with half-width of 5 cm^{-1} were used. See Tables 2 and 3 for vibrational mode numbering.

In order to account for basis set truncation, electron-correlation effects and vibrational anharmonicity, the calculated harmonic wavenumbers (ω) of all normal modes were corrected through a commonly employed scaling procedure [44,45]. In the present case we used a single scaling factor of 0.9594, recently obtained by Irikura et al. [46] for the B3LYP/6-31G* level of calculation, by means of a least-mean squared fitting procedure using a group of 3310 observed and computed vibrational ω values. For the reference compound naphthalene this approach has given a satisfactory agreement with experiment, with a rms deviation of 16 cm^{-1} [47], while the corresponding rms value for unscaled ω values is 62 cm^{-1}. Fig. 2 depicts the computed infrared spectrum in the 500–1800 cm^{-1} range for both isomers, obtained by convoluting the ω values with Lorentz lineshapes with half-width of 5 cm^{-1}. Vibrational modes were assigned on the basis of normal modes as displacements in redundant internal coordinates (in GAUSSIAN 03, option Freq = IntModes) as well as through the visualization software Chemcraft [48]. The complete lists of the ω and I_{IR} data for 1,6-DNB*a*P and 3,6-DNB*a*P isomers are reported in Tables 2 and 3, respectively. However, a detailed discussion of IR spectrum of the DNB*a*P isomers is beyond the aim of the present study. As can be appreciated from Fig. 2 and from data in Tables 2 and 3, the computed infrared spectrum of the investigated isomers is somewhat similar to each other, confirming the results previously obtained on the structure. For both the isomers, the most intense absorption is placed at ca. 1320 cm^{-1} and is mainly ascribed to the N—C stretching + symmetric O—N—O stretching vibration of the nitro groups in 1 and 3 positions (mode ν_{31} for both isomers), in line with experimental and computed infrared ω data of 1-, 3-, and 6-NB*a*P isomers, being in the range of 1310–1388 cm^{-1} [13,24]. It should be noted that ν_{31} vibration is about twice more intense than the corresponding mode principally localized on the nitro group in position 6 (mode ν_{27} and ν_{28}, for 1,6-DNB*a*P and 3,6-DNB*a*P, respectively) which occurs at higher ω value (by ca. 30 cm^{-1}), as can be also appreciated from Fig. 2. This result is supported by the computed

Table 2
Harmonic vibrational wavenumber, ω (cm^{-1}) and infrared intensity, I_{IR} (km/mol) of 1,6-dinitrobenzo[*a*]pyrene

No.	ω^a	I_{IR}	No.	ω^a	I_{IR}
1	3149.2	4.7	52	917.2	0.4
2	3122.0	0.8	53	896.2	4.6
3	3120.0	3.0	54	858.0	22.5
4	3115.9	6.4	55	842.3	36.3
5	3112.3	16.4	56	838.6	1.1
6	3093.3	1.8	57	814.9	72
7	3080.9	20.3	58	808.5	39.9
8	3073.9	13.1	59	793.3	6.1
9	3067.6	3.3	60	789.2	20.8
10	3067.3	5.5	61	776.1	2.1
11	1616.8	10.3	62	769.2	8.0
12	1601.4	1.6	63	752.4	28.9
13	1590.3	11.5	64	736.3	23.5
14	1577.3	163.9	65	725.9	6.5
15	1570.9	86.8	66	717.9	0.7
16	1558.5	101.2	67	695.2	6.5
17	1547.9	66.9	68	676.6	7.9
18	1533.0	22.2	69	661.3	0.9
19	1497.1	0.2	70	641.6	2.3
20	1478.8	45.8	71	634.0	4.8
21	1458.6	4.2	72	631.1	4.2
22	1440.3	15.4	73	582.7	1.3
23	1411.8	0.2	74	576.3	1.2
24	1395.3	3.3	75	543.9	1.4
25	1388.6	6.8	76	539.3	2.5
26	1366.3	21.3	77	525.0	2.2
27	1349.4	205.8	78	503.4	2.0
28	1346.2	4.5	79	500.2	1.9
29	1336.4	95.8	80	488.7	1.4
30	1328.6	102.5	81	460.9	2.1
31	1318.9	523.1	82	442.4	1.6
32	1301.0	43.5	83	437.3	0.4
33	1292.0	0.7	84	395.1	0.6
34	1245.7	30.6	85	361.8	1.8
35	1234.1	5.8	86	347.6	0.6
36	1225.7	7.2	87	317.8	1.3
37	1185.0	19.7	88	298.6	0.2
38	1172.8	28.1	89	291.3	0.0
39	1162.2	17.1	90	278.3	0.3
40	1152.2	0.7	91	233.3	4.0
41	1142.5	2.3	92	230.0	3.4
42	1121.3	18.9	93	206.5	0.9
43	1100.1	0.3	94	182.3	0.9
44	1040.5	18.6	95	157.1	1.3
45	1028.2	13.4	96	142.0	3.1
46	1014.3	1.9	97	99.1	1.3
47	957.8	0.1	98	92.0	0.4
48	953.5	0.5	99	70.4	1.5
49	945.2	0.4	100	60.2	1.1
50	944.4	0.1	101	44.4	0.5
51	934.8	2.0	102	37.0	3.3

B3LYP/6-31G* results.
[a] Values corrected for 0.9594 scaling factor taken from Ref. [46].

APT charge over the nitro groups (qNO$_2$) obtained through calculations of dipole moment derivatives (q_i(APT) is the atomic charge of the *i*th atom [34,35]):

$$q_i(\mathrm{APT}) = \frac{1}{3}\left(\frac{\partial \mu_x}{\partial x_i} + \frac{\partial \mu_y}{\partial y_i} + \frac{\partial \mu_z}{\partial z_i}\right) \quad (3)$$

As reported in the literature, dipole moment derivatives can be estimated experimentally from infrared intensities and can be accurately determined by means of quantum-mechanical computations [34,35,49]. For the nitro group in positions 1 and 3, B3LYP/6-31G* qNO$_2$(APT) value is substantially negative, being calculated to be −0.134 and −0.129 e, respectively. By contrast, the corresponding value for nitro substituent in position 6 is only slightly negative being −0.027 and −0.017 e, for 1,6-DNB*a*P and 3,6-DNB*a*P isomer, respectively. It implies for this nitro group

Table 3
Harmonic vibrational wavenumber, ω (cm^{-1}) and infrared intensity, I_{IR} (km/mol) of 3,6-dinitrobenzo[*a*]pyrene

No.	ω^a	I_{IR}	No.	ω^a	I_{IR}
1	3150.0	4.6	52	918.0	13.4
2	3123.0	1.1	53	913.5	1.1
3	3116.9	7.3	54	850.5	26.5
4	3115.3	3.5	55	838.6	1.9
5	3115.2	18.6	56	831.6	32.0
6	3096.2	2.8	57	817.7	32.8
7	3081.2	20.6	58	808.6	31.7
8	3073.1	12.1	59	789.7	24.0
9	3067.5	5.4	60	787.6	5.8
10	3064.2	3.4	61	775.4	1.6
11	1612.8	11.8	62	765.7	28.7
12	1601.2	3.5	63	749.9	31.0
13	1593.8	7.4	64	734.5	26.8
14	1577.1	154.6	65	728.5	6.0
15	1571.0	196.2	66	716.7	2.0
16	1560.2	30.5	67	701.2	6.3
17	1548.2	25.0	68	677.6	8.1
18	1535.8	33.2	69	661.8	0.3
19	1496.5	15.7	70	652.6	3.6
20	1477.9	6.2	71	633.1	5.8
21	1454.7	4.4	72	610.3	1.0
22	1445.0	28.4	73	590.3	1.4
23	1403.1	0.7	74	580.1	1.7
24	1400.2	4.0	75	543.3	0.2
25	1391.4	8.6	76	532.6	2.1
26	1364.8	14.5	77	522.8	2.2
27	1353.2	18.0	78	503.1	0.7
28	1349.8	243.4	79	502.1	3.5
29	1335.6	128.3	80	490.3	1.2
30	1327.7	15.9	81	472.2	0.4
31	1322.9	432.9	82	443.1	1.6
32	1305.6	68.3	83	424.2	3.0
33	1290.7	10.7	84	400.0	0.7
34	1244.8	15.0	85	363.2	0.8
35	1239.2	3.6	86	351.3	0.6
36	1216.1	14.2	87	315.5	0.6
37	1180.1	18.1	88	295.6	0.4
38	1170.7	37.9	89	286.6	3.0
39	1163.7	0.4	90	272.8	0.8
40	1150.9	6.8	91	232.9	3.4
41	1148.3	1.0	92	224.1	3.7
42	1121.4	14.2	93	209.5	1.0
43	1101.7	1.8	94	199.5	2.8
44	1041.9	17.1	95	154.5	0.8
45	1025.7	2.7	96	136.5	0.5
46	1008.8	6.6	97	100.2	0.4
47	962.8	0.3	98	85.6	1.7
48	957.1	0.1	99	76.4	1.3
49	940.0	0.0	100	62.5	1.9
50	938.3	9.8	101	47.2	0.5
51	929.6	0.3	102	34.0	0.1

B3LYP/6-31G* results.
[a] Values corrected for 0.9594 scaling factor taken from Ref. [46].

smaller dipole moment derivatives with respect to the normal mode coordinates (note that $I_{IR} \propto \partial\mu/\partial Q$ [34]) and lower electronic charge-transfer from the π-system of the B*a*P moiety in comparison to the substituents in 1 and 3 positions, in line with structural data. Note that the N—C stretching + asymmetric O—N—O stretching vibrations (modes ν_{14} and ν_{15}), which for both isomers are located at ca. 1570 cm^{-1}, (observed and calculated infrared ω values for NB*a*P isomers are in the range of 1511–1547 cm^{-1} [13,24]) 1–3 times less intense than the corresponding symmetrical vibrations.

3.3. Ionization potential and electron affinity

It is widely recognized that oxidation and reduction reactions and/or their combinations may take part in the metabolic mutagenic pathways, playing a fundamental role in the different mutagenic behaviour of NPAH isomers [2,3,10,11]. Therefore it is of interest to investigate oxidative and reductive capacities of DNB*a*P isomers. This can be achieved through estimation of IP and EA values or of their approximate counterparts, that are, highest occupied molecular orbital (HOMO) and lowest unoccupied molecular orbital (LUMO) eigenvalues (ε_{HOMO} and ε_{LUMO}, respectively). On the basis of the Koopmans' theorem [50], ε_{HOMO} and ε_{LUMO} can be related to the first ionization potential ($IP \approx -\varepsilon_{HOMO}$) and electron affinity ($EA \approx -\varepsilon_{LUMO}$). Calculated ε_{LUMO} values were previously employed to elucidate mutagenic potencies of large series of NPAHs with different molecular size and structure within Quantitative Structure Activity Relationships (QSARs) approaches [11,51,52]. However it is well known that ε_{LUMO} value can be significantly affected by the theoretical method, and caution should be used when choosing the level of computation. Previous ε_{LUMO}/mutagenic activity QSARs studies often employed ε_{LUMO} values obtained at semiempirical levels [11,51,52], which for some cases gave inadequate EA estimations. In fact, for the prototypical nitronaphthalene (NN) isomers, AM1 ε_{LUMO} values were calculated to be −1.266 and −1.415 eV for 1-NN and 2-NN isomers, respectively, [11], in disagreement with the observed EA values of 1.23 and 1.18 eV, respectively [53]. In addition, for the different mutagenic 3-NB*a*P and 6-NB*a*P isomers, AM1 predicts almost similar ε_{LUMO} values of −1.766 and −1.767 eV, respectively [11], in disagreement with recent B3LYP/6-31+G* ΔSCF computations which give EA values of 1.55 and 1.34 eV, respectively [54].

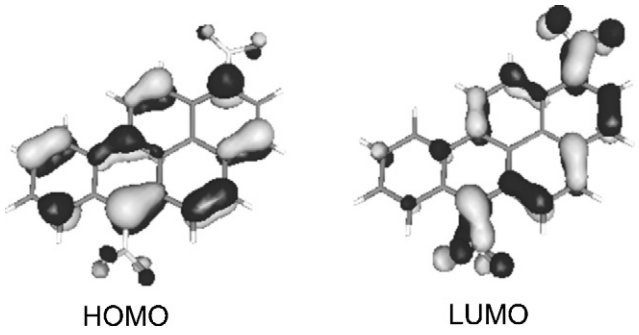

Fig. 3. HF/6-31+G* HOMO and LUMO of 1,6-dinitrobenzo[*a*]pyrene.

Table 4 reports computed IP, EA, ε_{HOMO} and ε_{LUMO} of DNB*a*P isomers, together with the values of the reference compounds NB and B*a*P, for which some experimental data are available from the literature. For NB and B*a*P observed IP values were obtained from photoelectron spectroscopy [55,56], while EA figures were estimated from ion–molecule reaction equilibrium method [57] and laser photoelectron spectroscopy measurements [58]. So far, experimental IP and EA values of DNB*a*Ps are unavailable. As can be seen from the data reported in Table 4, in the case of NB, a satisfactory agreement is found between observed [55,58] and computed IP and EA values, with deviations of 0.07 and 0.12 eV, respectively. On the other hand, for B*a*P present B3LYP/6-31+G* calculations underestimates the experimental IP [56] and EA [57] figures by 0.36 and 0.14 eV, respectively.

Fig. 3 shows a graphical representation of the HOMO for 1,6-DNB*a*P isomer, as supplied by the HF/6-31+G* computations. An analogue picture (here not reported) is also obtained for 3,6-DNB*a*P isomer. The results show that, π-like HOMO is essentially delocalized over the B*a*P framework and ε_{HOMO} value is computed to be almost the same for both the DNB*a*P isomers. This finding is also confirmed by the IP value which is calculated to be ca. 7.7 eV for both the isomers. Introduction of the two nitro groups increases the IP value of the B*a*P moiety by about 1 eV, implying a less pronounced tendency for DNB*a*Ps to oxidation in comparison to B*a*P.

Table 4
First ionization potential, IP (eV), electron affinity, EA (eV), HOMO and LUMO eigenvalues, ε_{HOMO} (eV) and ε_{LUMO} (eV), hardness, η (eV), electrophilic index, κ (eV), dipole moment, μ (D) and static electronic averaged polarizabity, $\langle\alpha\rangle$ (a.u.), of dinitrobenzo[*a*]pyrene isomers, benzo[*a*]pyrene and nitrobenzene[a]

	1,6-DNB*a*P	3,6-DNB*a*P	B*a*P		NB	
	Calculated	Calculated	Calculated	Experimental	Calculated	Experimental
IP	7.71	7.70	6.76	7.12[b]	9.99	9.92[c]
EA	2.19	2.15	0.67	0.81[d]	0.88	1.00[e]
ε_{HOMO}[f]	−7.95	−7.92	−6.77		−10.10	
ε_{LUMO}[f]	−0.42	−0.37	1.16		0.86	
η[g]	2.76	2.78	3.05	3.16	4.56	4.46
κ[h]	4.44	4.37	2.27	2.49	3.24	3.34
μ	1.91 (1.52)	8.17 (8.85)	0.01 (0.01)		4.96 (5.35)	4.22[i]
$\langle\alpha\rangle$	(304.0)	(304.3)	(257.1)		(85.8)	87.0[j]; 90.4[k]

[a] Values are obtained at the B3LYP/6-31+G* level on the B3LYP/6-31G* geometry of the ground state. Value in parentheses refers to PM6 calculations.
[b] Photoelectron spectroscopy, Ref. [56].
[c] Photoelectron spectroscopy, Ref. [55].
[d] Ion–molecule reaction equilibrium method, Ref. [57].
[e] Laser photoelectron spectroscopy, Ref. [58].
[f] Values are obtained at the HF/6-31+G* level on the B3LYP/6-31G* geometry of the ground state.
[g] Data obtained through equation (9) using IP and EA values.
[h] Data obtained through equation (10) using IP and EA values.
[i] Gas-phase, Ref. [69].
[j] DMSO solution, Ref. [72].
[k] Hexane solution, Ref. [72].

As should be expected, due to the presence of the strong withdrawal nitro substituents, for both DNB*a*Ps, anionic state lies at rather lower energy than the neutral ground state, giving EA value noticeably positive. Despite for 3,6-DNB*a*P isomer reduction reactions give a larger amount of nitroso- and amino-derivative mutagenic intermediates than 1,6-DNB*a*P isomer [18], EA value does not change between the investigated isomers, being calculated to be ca. 2.2 eV. This result is also confirmed by the ε_{LUMO} data. Present EA and ε_{LUMO} data are consistent with electrochemical reduction potentials involving the transfer of two electrons previously obtained through cyclic voltammetry measurements [15], being −0.65 and −0.67 V for 1,6-DNB*a*P and 3,6-DNB*a*P, respectively. Differently, we note that for NB*a*Ps isomers, where mutagenic activity increases in the order 6-NB*a*P < 1-NB*a*P ∼ 3-NB*a*P, B3LYP/6-31+G* ΔSCF EA value varies, being 1.34, 1.58, 1.55 eV, respectively [54]. As can be appreciated from Fig. 3, LUMO of 1,6-DNB*a*P isomer is principally localized on both the nitro substituents exhibiting a remarkable π density along the C—N bonds (note that a similar situation is also found for 3,6-DNB*a*P isomer). However, while the electronic density over the C—N bond in 1 and 3 positions is presumed to give a bonding contribution, that in position 6 should yield a somewhat destabilizing effect to LUMO. These results are supported by the computed atomic charges (qNO$_2$) and spin densities (δ_sNO$_2$) over the nitro groups of the anionic state, obtained at the UB3LYP/6-31+G* level and reported in Table 5. Indeed, for the nitro group in positions 1 and 3, qNO$_2$ is more negative than the corresponding value in position 6 by 15–30%, depending on the population scheme employed (Mulliken, ESP, NBO). Additionally, δ_sNO$_2$ value in position 6 (0.14) is somewhat lower than that in 1 (0.22) and 3 (0.21) position. As a consequence, for the neutral species, nitro group in position 6 is less susceptible to reduction than that in positions 1 and 3, in agreement with previous experimental results [15]. Introduction of the two nitro groups increases EA value of the B*a*P moiety by ca. 1.5 eV, implying a better tendency of DNB*a*Ps to reduction reactions with respect to B*a*P and NB*a*Ps, in agreement with experimental findings [18]. The above results on EA values clearly indicate that, the different mutagenic activity of 1,6-DNB*a*P and 3,6-DNB*a*P isomers, which is predicted to be up to 1–2 orders of magnitude [15–18], cannot be directly related to the reductive capacity of these isomers.

Table 5
Mulliken, ESP and NBO atomic charge, q (e), and Mulliken spin density, δ_s, over NO$_2$ groups of dinitrobenzo[*a*]pyrene isomers in their anionic state[a]

	1,6-DNB*a*P		3,6-DNB*a*P	
	$(NO_2)'$[b]	$(NO_2)''$[c]	$(NO_2)'$[b]	$(NO_2)''$[c]
q (Mulliken)	−0.565	−0.480	−0.550	−0.477
q (ESP)	−0.359	−0.298	−0.371	−0.252
q (NBO)	−0.475	−0.381	−0.466	−0.379
δ_s (Mulliken)	0.218	0.137	0.215	0.138

[a] Values are obtained at the UB3LYP/6-31+G* level on the B3LYP/6-31G* geometry of the ground state.
[b] Value calculated over O_{22}–N_{21}–O_{23} group. See Fig. 1 for atomic numbering.
[c] Value calculated over O_{24}–N_{25}–O_{26} group. See Fig. 1 for atomic numbering.

Physicochemical properties widely used in the literature such as hardness (η) and electrophilicity index (κ), which give a measure of stability and reactivity of molecules, can be estimated from the computed IP and EA values through finite-difference expressions [59]. Not surprisingly, η and κ values (see Table 4) are almost identical for DNB*a*P isomers, and are consistent with the maximum hardness principle [60], which establishes that isoenergetic isomers should have almost the same η value. It is of interest to note that, the electrophilicity increases in the order B*a*P < NB < 3,6-DNB*a*P ∼ 1,6-DNB*a*P, and is mainly determined by the EA value.

3.4. Dipole moments and electronic polarizabilities

Besides the evaluation of IP and EA values which are related to oxidative and reductive processes, respectively, it is of interest to investigate the effects of the position of the nitro substituents on some important chemical–physical properties such as μ and α. Previous studies have demonstrated that permanent and induced electric properties such as dipole moment, quadrupole moment and electronic (hyper) polarizabilities may play an important role in intermolecular interactions, determining binding affinity in enzyme-substrate complexes, through electrostatic, inductive and dispersive contributions [25,43,47,54,61–67]. In particular, electric properties of homologue series of polychlorinated dibenzo-*p*-dioxins and polychlorinated dibenzofurans were previously employed to elucidate the congener specific toxicities, which are supposed to be dependent on ligand–receptor binding capabilities [61–67]. It should be mentioned that enzyme–substrate interac-

tions were hypothesized to be important steps in the proposed mutagenic pathways of NPAHs, preceding nitroreductive reactions [10,11]. Additionally, there are some indications showing that electronic polarizability might be related to hydrophobicity [68], which was found to be crucial for the description of the mutagenic activity of a large series of NPAH compounds [11,51]. Recently, the different mutagenic behaviour of NN and NB*a*P isomers has been also elucidated on the basis of their permanent and induced electronic charge distributions [43,54].

Table 4 presents μ and static electronic <α> values of DNB*a*P isomers, together with the data of B*a*P and NB for which some experimental values are available from the literature. Both the B3LYP/6-31+G* and PM6 μ values of NB overestimate the observed gas-phase value of 4.22 D [69] by 18% and 27%, respectively. However, the B3LYP/6-31+G* μ value of 4.96 D is quite close to recent high-level theoretical estimate of 4.78 D [70], obtained at B3LYP/aug-cc-pVTZ level. As can be appreciated from Fig. 1 and data of Table 4, on passing from 1,6-DNB*a*P to 3,6-DNB*a*P isomer μ value increases by about 4 times. Analysis of the vectorial contributions from the individual nitro groups is helpful to elucidate the above result. In the case of 1,6-DNB*a*P isomer, the nitro substituents are essentially in mutual opposition to each other. As a consequence, their dipolar contributions tend to cancel to each other, giving at the B3LYP/6-31+G* level a μ value of 1.91 D. On the contrary, for 3,6-DNB*a*P the μ value is predicted to be much more greater than that of 1,6-DNBaP isomer, being computed at 8.17 D. This large μ value can be attributed to the additive contribution from both the nitro groups. The above difference in dipole moment between DNB*a*P isomers might be the origin of their different mutagenic behaviour, supporting enzyme–substrate complex formation as fundamental step in the metabolic activation of these nitroaromatics. It is of interest to note that, owing to the greater distance between positive (hydrocarbon moiety) and negative (nitro group) charges, 3,6-DNB*a*P isomer is more polar than the typical charge-transfer organic molecule of *p*-nitroaniline, for which an experimental μ value of 6.29 D obtained in benzene solution was previously reported [71].

Table 4 also includes the static electronic <α> values of the investigated compounds computed at the PM6 level on the B3LYP/6-31G* geometry. As can be seen from the Table, PM6 computations reproduce satisfactorily well the experimental values of NB obtained in both DMSO and hexane solutions [72] with a difference of 1.2 a.u. (−1.4%) and 4.6 a.u. (−5.1%), respectively. In addition present PM6 <α> datum agrees reasonably well with the previous high-level theoretical MP2/[5s3p2d/3s2p] prediction of 88.3 a.u. [73], with a deviation of −2.8%. Note that, introduction of the two nitro groups increases the <α> value of B*a*P by ca. 50 a.u. (ca. 20%). Differently from μ, and in agreement with the computed molar volumes, <α> value remains almost unchanged on passing from 1,6-DNB*a*P to 3,6-DNB*a*P isomer being computed within 0.3 a.u., suggesting that their dispersive effects are expected to be comparable. Also note that, 1,6-DNB*a*P and 3,6-DNB*a*P isomers show an identical hydrophobic character as predicted by the octanol/water partition coefficient values obtained by means of the ALOGPS 2.1 program [74–76], in some consistency with the polarizability values. Finally, one notices that the analogue <α> value for the investigated DNB*a*P isomers is in line with the above energetic and structural properties, in agreement with the minimum polarizability principle [77] and maximum hardness principle [60].

4. Conclusions

The molecular structures, vibrational spectra and electronic properties of 1,6-DNB*a*P to 3,6-DNB*a*P isomers have been studied by using DFT-B3LYP and semiempirical PM6 levels of calculation. Present results suggest that, the different mutagenic activities of the investigated DNB*a*P isomers might be ascribed to the different binding affinity with enzymes involved in the mutagenic pathways. In particular, electrostatic and inductive interactions, which are dependent on the electronic charge distribution of the interacting units, are expected to give an essential contribution to formation of enzyme-DNB*a*P complexes, especially in the case of 3,6-DNB*a*P isomer. On the other hand, our data show that the specific geometrical characteristics of the nitro substituents, the molecular bulk, as well as reductive and oxidative features are somewhat similar between 1,6-DNB*a*P and 3,6-DNB*a*P isomers, and consequently are presumed not to contribute to the different mutagenic behaviour of the investigated isomers. Present computational approaches might be useful to elucidate and predict mutagenic potencies of other series of NPAH isomers, for which data are not yet available.

Acknowledgement

Work partially supported by MIUR, Rome.

References

[1] J.N. Pitts, K.A. Van Cauwenberghe, D. Grosjean, J.P. Schmid, D.R. Fits, W.L. Belser, G.B. Knudson, P.M. Hynds, Atmospheric reactions of polycyclic aromatic hydrocarbons: facile formation of mutagenic nitro derivatives, Science 202 (1978) 515–519.
[2] H. Tokiwa, Y. Ohnishi, Mutagenicity and carcinogenicity of nitroarenes and their sources in the environment, Crit. Rev. Toxicol. 17 (1986) 23–60.
[3] P.P. Fu, Metabolism of nitro-polycyclic aromatic hydrocarbons, Drug Metab. Rev. 22 (1990) 209–268.
[4] M.G. Nishioka, C.C. Howard, D.A. Contos, L.M. Ball, J. Lewtas, Detection of hydroxylated nitro aromatic and hydroxylated nitro polycyclic aromatic compounds in an ambient air particulate extract using bioassay-directed fractionation, Environ. Sci. Technol. 22 (1988) 908–915.
[5] L.A. Gundel, J.M. Dalsey, L.R.F. de Carvalho, N.Y. Kado, D. Schuetzle, Polar organic matter in airborne particles: chemical characterization and mutagenic activity, Environ. Sci. Technol. 27 (1993) 2112–2119.
[6] T. Enya, H. Suzuki, T. Watanabe, T. Hirayama, Y. Hisamatsu, 3-Nitrobenzanthrone, a powerful bacterial mutagen and suspected human carcinogen found in diesel exhaust and airborne particulates, Environ. Sci. Technol. 31 (1997) 2772–2776.
[7] J.C. Spain, Biodegradation of nitroaromatic compounds, Ann. Rev. Microbiol. 49 (1995) 523–555.
[8] R.E. Parales, J.L. Ditty, Laboratory evolution of catabolic enzymes and pathways, Curr. Opin. Biotechnol. 16 (2005) 315–325.
[9] R. Friemann, M.M. Ivkovic-Jensen, D.J. Lessner, C.-L. Yu, D.T. Gibson, R.E. Parales, H. Eklund, S. Ramaswamy, Structural insight into dioxygenation of nitroarene compounds: crystal structure of nitrobenzene dioxygenase, J. Mol. Biol. 348 (2005) 1139–1151.
[10] W.A. Vance, H.S. Okamoto, Y.Y. Wang, Structural features of nitroaromatics and their reduction products that affect mutagenic potency in the Ames Salmonella assay, in: C.M. King, L.J. Romano, D. Schuetzle (Eds.), Carcinogenic and Mutagenic Responses to Aromatic Amines and Nitroarenes, Elsevier, New York, 1988, pp. 291–302.
[11] A.K. Debnath, R.L. Lopez de Compadre, G. Debnath, A.J. Shusterman, C. Hansch, Structure-activity relationship of mutagenic aromatic and heteroaromatic nitro compounds. Correlation with molecular orbital energies and hydrophobicity, J. Med. Chem. 34 (1991) 786–797.
[12] V. Purohit, A.K. Basu, Mutagenicity of nitroaromatic compounds, Chem. Res. Toxicol. 13 (2000) 673–692.
[13] Y.S. Li, P.P. Fu, J.S. Church, The conformation of some nitro-polycyclic aromatic hydrocarbons, J. Mol. Struct. 550–551 (2000) 217–223, and references therein.
[14] J.N. Pitts Jr., D.M. Lokensgard, W. Harger, T.S. Fisher, V. Mejia, J.J. Schuler, G.M. Scorziell, Y.A. Katzenstein, Mutagens in diesel exhaust particulate. Identification and direct activities of 6-nitrobenzo[*a*]pyrene, 9-nitroanthracene,1-nitropyrene and 5h-phenanthro[4,5-bcd]pyran-5-one, Mutat. Res. 103 (1982) 241–249.
[15] K. Fukuhara, N. Miyata, M. Matsui, K. Matsui, M. Ishidate Jr., S. Kamiya, Synthesis, chemical properties and mutagenicity of 1,6- and 3,6-dinitrobenzo[*a*]pyrenes, Chem. Pharm. Bull. 38 (1990) 3158–3161.
[16] N. Sera, M. Kai, K. Horikawa, K. Fukuhara, N. Miyata, H. Tokiwa, Detection of 3,6-dinitiro-benzo[*a*]pyrene in airborne particulates, Mutat. Res. 263 (1991) 27–32.
[17] N. Sera, K. Fukuhara, N. Miyata, K. Horikawa, H. Tokiwa, Mutagenicity of nitroazabenzo[*a*]pyrene and its related compound, Mutat. Res. 280 (1992) 81–85.

[18] H. Tokiwa, N. Sera, A. Nakashima, K. Nakashima, Y. Nakanishi, N. Shigematu, Mutagenic and carcinogenic significance and the possible induction of lung cancer by nitro aromatic hydrocarbons in particulate pollutants, Environ. Health Perspect. 102 (1994) 107–110.
[19] K. Horikawa, N. Sera, K. Murakami, N. Sano, K. Izumi, H. Tokiwa, Comparative tumorigenicity of 1- and 3-nitrobenzo[*a*]pyrenes, and 3,6- and 1,6-dinitrobenzo[*a*]pyrenes in F344/DuCrj rats, Toxicol. Lett. 98 (1998) 51–58.
[20] S. Ishii, Y. Hisamatsu, K. Inazu, T. Kobayashi, K. Aika, Mutagenic nitrated benzo[*a*]pyrene derivatives in the reaction product of Benzo[*a*]pyrene in NO_2-air in the presence of O_3 or under photoirradiation, Chemosphere 41 (2000) 1809–1819.
[21] N. Sera, K. Fukuhara, N. Miyata, H. Tokiwa, Detection of nitro-azabenzo[*a*]pyrene derivatives in the semivolatile phase originating from airborne particulate matter, diesel and gasoline vehicles, Mutagenesis 9 (1994) 47–52.
[22] S.D. Warner, A.-M. Lebuis, J.-P. Farant, I.S. Butler, Crystal structure of 6-nitrobenzo(*a*)pyrene, J. Chem. Cryst. 33 (2003) 213–217.
[23] R.G. Parr, W. Yang, Density Functional Theory of Atoms and Molecules, Oxford University Press, New York, 1989.
[24] K.K. Onchoke, C.M. Hadad, P.K. Dutta, Structure and vibrational spectra of mononitrated benzo[*a*]pyrenes, J. Phys. Chem. A 110 (2006) 76–84.
[25] V. Librando, A. Alparone, Electronic polarizability as a predictor of biodegradation rates of dimethylnaphthalenes. An ab initio and density functional theory study, Environ. Sci. Technol. 41 (2007) 1646–1652.
[26] MOPAC 2007, J.J.P. Stewart, Stewart Computational Chemistry, Colorado Springs, CO, USA, 2007, http://OpenMOPAC.net.
[27] M.J. Frisch, G.W. Trucks, H.B. Schlegel, G.E. Scuseria, M.A. Robb, V.G. Cheeseman, J.A. Montgomery, T. Vreven Jr., K.N. Kudin, J.C. Burant, J.M. Millam, S.S. Iyengar, J. Tomasi, V. Barone, B. Mennucci, M. Cossi, G. Scalmani, N. Rega, G.A. Petersson, H. Nakatsuji, M. Hada, M. Ehara, K. Toyota, R. Fukuda, J. Hasegawa, M. Ishida, T. Nakajima, Y. Honda, O. Kitao, H. Nakai, M. Klene, X. Li, J.E. Knox, H.P. Hratchian, J.B. Cross, C. Adamo, J. Jaramillo, R. Gomperts, R.E. Stratmann, O. Yazyev, A.J. Austin, R. Cammi, C. Pomelli, J.W. Ochterski, P.Y. Ayala, K. Morokuma, G.A. Voth, P. Salvador, J.J. Dannenberg, V.G. Zakrzewski, S. Dapprich, A.D. Daniels, M.C. Strain, O. Farkas, D.K. Malick, A.D. Rabuck, K. Raghavachari, J.B. Foresman, J.V. Ortiz, Q. Cui, A.G. Baboul, S. Clifford, J. Cioslowski, B.B. Stefanov, G. Liu, A. Liashenko, P. Piskorz, I. Komaromi, R.L. Martin, D.J. Fox, T. Keith, M.A. Al-Laham, C.Y. Peng, A. Nanayakkara, M. Challacombe, P.M.W. Gill, B. Johnson, W. Chen, M.W. Wong, C. Gonzalez, J.A. Pople, GAUSSIAN 03, revision B.03, Gaussian, Inc., Pittsburgh, PA, 2003.
[28] J.J.P. Stewart, Optimization of parameters for semiempirical methods V: modification of NDDO approximations and application to 70 elements, J. Mol. Model. 13 (2007) 1173–1213.
[29] A.D. Becke, A new mixing of Hartree-Fock and local density-functional theories, J. Chem. Phys. 98 (1993) 1372–1377.
[30] C. Lee, A.D. Yang, R.G. Parr, Development of the Colle–Salvetti correlation-energy formula into a functional of the electron density, Phys. Rev. B 37 (1988) 785–789.
[31] W.J. Hehre, L. Random, P.v.R. Schleyer, J.A. Pople, Ab Initio Molecular Orbital Theory, Wiley, New York, 1986.
[32] A. Modelli, L. Mussoni, D. Fabbri, Electron affinities of polycyclic aromatic hydrocarbons by means of B3LYP/6-31+G calculations, J. Phys. Chem. A 110 (2006) 6482–6486.
[33] A. Modelli, D. Jones, Temporary anion states and dissociative electron attachment to isothiocyanates, J. Phys. Chem. A 110 (2006) 13195–13201.
[34] W.B. Person, G. Zerbi (Eds.), Vibrational Intensities in Infrared and Raman Spectroscopy, Elsevier Scientific Publishing Co., New York, 1982.
[35] J. Cioslowski, A new population analysis based on atomic polar tensors, J. Am. Chem. Soc. 111 (1989) 8333–8336.
[36] B.H. Besler, K.M. Merz Jr., P.A. Kollman, Atomic charges derived from semiempirical methods, J. Comput. Chem. 11 (1990) 431–439.
[37] NBO Version 3.1, E.D. Glendening, A.E. Reed, J.E. Carpenter, F. Weinhold.
[38] H. Sekino, R.J. Bartlett, Frequency dependent nonlinear optical properties of molecules, J. Chem. Phys. 85 (1986) 976–989.
[39] F. Sim, S. Chin, M. Dupuis, J.E. Rice, Electron correlation effects in hyperpolarizabilities of *p*-nitroaniline, J. Phys. Chem. 97 (1993) 1158–1163, and references therein.
[40] J. Iball, S.N. Scrimgeour, D.W. Young, 3,4-Benzopyrene (a new refinement), Acta Cryst. B 32 (1976) 328–330.
[41] K.K. Onchoke, C.M. Hadad, P.K. Dutta, Density functional theoretical study of nitrated polycyclic aromatic hydrocarbons, Polycycl. Arom. Comp. 24 (2004) 37–64.
[42] L. Türker, T. Atalar, Ab initio and DFT study on 1,4-dinitroglycoluril configurational isomers: *cis*-DINGU and *trans*-DINGU, J. Hazard. Mater. A 137 (2006) 47–56.
[43] V. Librando, A. Alparone, Prediction of mutagenic activity of nitronaphthalene isomers by infrared and Raman spectroscopy, J. Hazard. Mater. 154 (2008) 1158–1165.
[44] P. Pulay, G. Fogarasi, G. Pongor, J.E. Boggs, A. Vargha, Combination of theoretical ab initio and experimental information to obtain reliable harmonic force constants. Scaled quantum mechanical (QM) force fields for glyoxal, acrolein, butadiene, formaldehyde, and ethylene, J. Am. Chem. Soc. 105 (1983) 7037–7047.
[45] G. Rauhut, P. Pulay, Transferable scaling factors for density functional derived vibrational force fields, J. Phys. Chem. 99 (1995) 3093–3100, and references therein.
[46] K.K. Irikura, R.D. Johnson, R.N. Kacker, Uncertainties in scaling factors for ab initio vibrational frequencies, J. Phys. Chem. A 109 (2005) 8430–8437.
[47] V. Librando, A. Alparone, Structure, vibrational properties and polarizabilities of methylnaphthalene isomers: a quantum-mechanical approach, Polycycl. Arom. Comp. 27 (2007) 65–94.
[48] G.A. Zhurko, D.A. Zhurko, Chemcraft, http://www.chemcraftprog.com.
[49] A.E. Oliveira, R.L.A. Haiduke, R.E. Bruns, Atomic mean dipole moment derivatives and GAPT charges, J. Phys. Chem. A 104 (2000) 5320–5327.
[50] T. Koopmans, Ordering of wave functions and eigenenergies to the individual electrons of an atom, Physica 1 (1933) 104–113.
[51] R.L. Lopez de Compadre, A.J. Shusterman, C. Hansch, The role of hydrophobicity in the Ames test. The correlation of the mutagenicity of nitropolycyclic hydrocarbons with partition coefficients and molecular orbital indices, Int. J. Quantum Chem. 34 (1988) 91–101.
[52] T. Takamura-Enya, H. Suzuki, Y. Hisamatsu, Mutagenic activities and physicochemical properties of selected nitrobenzanthrones, Mutagenesis 21 (2006) 399–404.
[53] T. Heinis, S. Chowdhury, P. Kebarle, Electron affinities of naphthalene, anthracene and substituted naphthalenes and anthracenes, Org. Mass. Spectrom. 28 (1993) 358–365.
[54] V. Librando, A. Alparone, G. Tomaselli, Electronic properties of some nitrobenzo[a]pyrene isomers: a possible relationship to mutagenic activity, J. Mol. Model. 14 (2008) 489–497.
[55] K. Kimura, S. Katsumata, Y. Achiba, T. Yamazaki, S. Iwata, Ionization energies, Ab initio assignments, and valence electronic structure for 200 molecules, in: Handbook of HeI Photoelectron Spectra of Fundamental Organic Compounds, Japan Scientific Soc. Press, Tokyo, 1981.
[56] I. Akiyama, K.C. Li, P.R. LeBreton, P.P. Fu, R.G. Harvey, Ultraviolet photoelectron studies of polycyclic aromatic hydrocarbons. The ground-state electronic structure of aryloxiranes and metabolites of benzo[*a*]pyrene, J. Phys. Chem. 83 (1979) 2997–3003.
[57] L. Crocker, T.B. Wang, P. Kebarle, Electron affinities of some polycyclic aromatic hydrocarbons, obtained from electron-transfer equilibria, J. Am. Chem. Soc. 115 (1993) 7818–7822.
[58] C. Desfrancois, V. Periquet, S.A. Lyapustina, T.P. Lippa, D.W. Robinson, K.H. Bowen, H. Nonaka, Compton electron binding to valence and multipole states of molecules: nitrobenzene, para- and meta-dinitrobenzenes, J. Chem. Phys. 111 (1999) 4569–4576.
[59] P.K. Chattaraj, U. Sarkar, D.R. Roy, Electrophilicity index, Chem. Rev. 106 (2006) 2065– 2091, and references therein.
[60] R.G. Pearson, The principle of maximum hardness, Acc. Chem. Res. 26 (1993) 250–255.
[61] J.D. McKinney, K.E. Gottschalk, L. Pedersen, The polarizability of planar aromatic systems. An application to polychlorinated biphenyls (PCB's), dioxins and polyaromatic hydrocarbons, J. Mol. Struct. (Theochem.) 105 (1983) 427–438.
[62] J.D. McKinney, Multifunctional receptor model for dioxin and related compound toxic action: possible thyroid hormone-responsive effector-linked site, Environ. Health Perspect. 82 (1989) 323–336.
[63] E. Fraschini, L. Bonati, D. Pitea, Molecular polarizability as a tool for understanding the binding properties of polychlorinated dibenzo-*p*-dioxins: definition of a reliable computational procedure, J. Phys. Chem. 100 (1996) 10564–10569.
[64] B.J. Mhin, J.E. Lee, W. Choi, Understanding the congener-specific toxicity in polychlorinated dibenzo-*p*-dioxins: chlorination pattern and molecular quadrupole moment, J. Am. Chem. Soc. 124 (2002) 144–148.
[65] R.S. Asatryan, N.S. Mailyan, L. Khachatryan, B. Dellinger, Electronic elasticity–toxicity relationships for polychlorinated dibenzo-*p*-dioxin congeners, Chemosphere 48 (2002) 227–236.
[66] S. Hirokawa, T. Imasaka, T. Imasaka, Chlorine substitution pattern, molecular electronic properties, and the nature of the ligand-receptor interaction: quantitative property-activity relationships of polychlorinated dibenzofurans, Chem. Res. Toxicol. 18 (2005) 232–238.
[67] C. Gu, X. Jiang, X. Ju, G. Yu, Y. Bian, QSARs for the toxicity of polychlorinated dibenzofurans through DFT-calculated descriptors of polarizabilities, hyperpolarizabilities and hyper-order electric moments, Chemosphere 67 (2007) 1325–1334.
[68] M. Karelson, V.S. Lobanov, A.R. Katritzky, Quantum-chemical descriptors in QSAR/QSPR studies, Chem. Rev. 96 (1996) 1027–1044, and references therein.
[69] C.P. Smyth, Dielectric Behaviour and Structure, McGraw-Hill, New York, 1955.
[70] S. Böhm, O. Exner, Dipole moments and electron distribution of conjugated molecules; para derivatives of benzene, J. Mol. Struct. (Theochem.) 803 (2007) 9–16.
[71] A.L. McClellan, Tables of Experimental Dipole Moments, Freeman, 1963.
[72] K.D. Singer, A.F. Garito, Measurements of molecular second order optical susceptibilities using dc induced second harmonic generation, J. Chem. Phys. 75 (1981) 3572–3580.
[73] R.H.C. Janssen, D.N. Theodorou, S. Raptis, M.G. Papadopoulos, Molecular simulation of static hyper-Rayleigh scattering: a calculation of the depolarization ratio and the local fields for liquid nitrobenzene, J. Chem. Phys. 111 (1999) 9711–9719.

[74] I.V. Tetko, J. Gasteiger, R. Todeschini, A. Mauri, D. Livingstone, P. Ertl, V.A. Palyulin, E.V. Radchenko, N.S. Zefirov, A.S. Makarenko, V.Y. Tanchuk, V.V. Prokopenko, Virtual computational chemistry laboratory-design and description, J. Comput. Aid. Mol. Des. 19 (2005) 453–463.
[75] VCCLAB, Virtual Computational Chemistry Laboratory, http://www.vcclab.org, 2005.
[76] I.V. Tetko, P. Bruneau, Application of ALOGPS to predict 1-octanol/water distribution coefficients, log P, and log D, of AstraZeneca in-house database, J. Pharm. Sci. 93 (2004) 3103–3110.
[77] P.K. Chattaraj, S. Sengupta, Popular electronic structure principles in a dynamical context, J. Phys. Chem. 100 (1996) 16126–16130.